Growth of preferentially-oriented AlN films on amorphous substrate by pulsed laser deposition

著者	Wang Z. P., Morimoto Akiharu, Kawae Takeshi, Ito H., Masugata Katsumi
journal or publication title	Physics Letters, Section A: General, Atomic and Solid State Physics
volume	375
number	33
page range	3007-3011
year	2011-08-01
URL	http://hdl.handle.net/2297/28987

doi: 10.1016/j.physleta.2011.06.043

ACCEPTED MANUSCRIPT

Growth of preferentially-oriented AlN films on amorphous substrate by pulsed laser deposition

Z.P. Wang[a*], A. Morimoto[b], T. Kawae[b], H. Ito[a], K. Masugata[a]

a Department of Electric and Electronic System Engineering, University of Toyama, 3190 Gofuku, Toyama 930-8555, Japan

b Graduate School of Natural Science and Technology, Kanazawa University, Kakuma-machi, Kanazawa, Ishikawa 920-1192, Japan

*Corresponding author: Tel.: +81-90-2099-8668, Fax: +81-76-445-6714; E-mail: wang_zhiping@yahoo.com

Abstract

Preferentially-oriented aluminum nitride (AlN) films are grown directly on natively-oxidized Si (100) substrate by pulsed laser deposition (PLD) in nitrogen (N_2) environment. The AlN preferential orientation changes from (002) to (100) with increasing N_2 pressure. Such different behaviors are discussed in terms of deposition-rate-dependent preferential orientation, kinetic energy of depositing species and confinement of laser plume. Finally, sample deposited at 0.9 Pa is proved to have the highest (002) peak intensity, the lowest FWHM value, the highest deposition rate and a relatively low RMS roughness (1.138 nm), showing the optimal growth condition for c-axis-oriented AlN growth at this N_2 pressure.

PACS classification codes: 81.15.Fg; 77.84.Bw ; 61.50Ks

Keyword: Pulsed laser deposition (PLD); Aluminum nitride (AlN); Nitrogen Pressure effects.

ACCEPTED MANUSCRIPT

Introduction

Aluminum nitride (AlN), with a wide direct band-gap (6.2 eV at 300 K) [1], high electrical resistance (10^9—10^{11}Ωm) [2], high thermal conductivity (up to 320 W/mK at room temperature) [3], a high acoustic propagation rate and a low transmission loss [4], offers tremendous potential for microelectronic devices, such as surface acoustic wave (SAW) devices [5], thin-film bulk acoustic resonators (FBARs) [6], contour mode resonators [7] and Lamb wave resonators [8, 9]. Compared to zinc oxide (ZnO), AlN films show a higher SAW velocity (5607 m/s instead of 2682 m/s), better mechanical properties (18 GPa instead of 5 Gpa in Vickers hardness) [10], resistance to humidity, and better endurance to chemical etching [11].

In SAW devices, the central frequency (f_0) is related to the spacing between the interdigital transducer (IDT) fingers (λ/4) and the propagation velocity on the substrate V_p by the simple formula: $f_0 = V_p/\lambda$ [12, 13]. In this sense, increased operation frequency of SAW devices can be achieved by using high-resolution IDT lithography (shorter λ) and/or high acoustic wave velocity materials as bottom layer. The first solution is highly required in terms of fabrication costs and precision; the second one is attractive if high-quality fast materials can be grown by standard thin film deposition techniques [14]. Amorphous diamond-like carbon is believed to be a good choice for bottom layer because of its highest propagating velocity among all materials [15].

Various techniques have been reported for the synthesis of AlN films, such as chemical vapor deposition [16], molecular beam epitaxy [17], ion-plating deposition

ACCEPTED MANUSCRIPT

[18] and reactive magnetron sputtering [19], etc. Most of these works report the epitaxial growth behaviors of AlN films on single-crystal substrates, few works can be found regarding the deposition of AlN on amorphous substrate. Pulsed laser deposition (PLD) is believed to be a good choice to grow high quality preferentially-oriented film on amorphous substrate. It is generally known that owing to the non-equilibrium nature of the process in PLD, the energetic species in the laser ablation plasma have a much higher kinetic energy (in the range of 10 - 100 eV) than that of conventional methods, like thermal evaporation process (~ 0.1 eV) [20]. Such energetic species would enhance the mobility of deposited adatoms and increase the film crystallinity on amorphous substrate.

To our knowledge, there is no report on the deposition of AlN film on amorphous substrate by PLD and the scope of this work is to fill this gap. As known, different crystal orientation of AlN films show different thermal expansion coefficient (c-axis parallel: 5.3×10^{-6} /K, a-axis parallel: 4.2×10^{-6} /K) [21] and different elastic constant (c_{11}=345 GPa and c_{33}=395 GPa) resulting in a different phase velocity [22]. In this study, we investigate the preferentially-oriented growth behavior of AlN film on amorphous substrate (silicon substrate with amorphous native oxide) and optimize the parameter of N_2 pressure for c-axis-oriented AlN growth. AlN films were later characterized by the X-ray diffractometer (XRD, RINT-2200, Rigaku), surface profilometer (Surfcom 1500DX, Tokyo Seimitsu), field-emission scanning electron microscopy (FE-SEM, JSM-6700F JEOL), and scanning probe microscope (SPM 9500 J2, Shimadzu).

ACCEPTED MANUSCRIPT

Experimental details

A second harmonic Q-switched Nd:YAG laser (Continuum, Surelite III-10M), operating at 532nm with 5 ns pulse duration, delivers a chosen energy of 380 mJ (corresponding to an energy density of 2 J/cm^2) at a repetition rate of 10 Hz. After two reflections, the laser beam was focused on a rotating sintered AlN target (99.999%) at 45° with respect to the normal direction of the target. During deposition, the target was continuously rotated around its center to ensure a complete elimination of stress and a fresh location for each incident laser pulse. The AlN target was polished before every experiment by mechanical abrasion, removing the topmost layer to preserve the target stoichiometry [23] and reduce the density of droplet often observed on PLD films. P-type Si (100) with a few nm thickness of native oxide layer was chosen as the substrate, because the (100) silicon is used in all CMOS electronics and is inexpensive. Prior to deposition, substrates were alternately cleaned in ultrasonic baths of deionized (DI) water and ethanol for several rounds to remove organic impurities and eventually dried with N_2 duster.

Target surface pre-ablation is necessary to remove impurities and to prevent droplets incorporation in the growing film. Thus, we block the first 3000 pulses by using a shutter between target and substrate. Afterwards, the shutter was removed and 6000 pulses were chosen for AlN film deposition. The physical properties of AlN films prepared by PLD mainly depend on the processing parameters such as substrate temperature, N_2 pressure, target substrate distance, laser pulse energy and pulse repetition rate. In the present experiment, for the sake of studying the influence of N_2

ACCEPTED MANUSCRIPT

pressure on AlN films growth, AlN films were deposited in a vacuum (evacuated up to ~10^{-4} Pa) and at N_2 pressures of 0.2 ~ 10 Pa, with fixed target-to-substrate distance of 50 mm and substrate temperature of 600℃.

Results and discussion

X-ray diffraction (XRD)

The crystalline structure and preferred orientation of the as-deposited films were characterized by XRD. Figure 1 shows the XRD patterns of AlN films deposited under various N_2 pressures. The diffraction peaks located at 2θ = 33.216°, 36.041 °and 59.350 ° are corresponding to (100), (002) and (110) of hexagonal AlN respectively (pdf no.: 25-1133). The strong diffraction peak at 2θ = 69° belongs to (400) of Si substrate. In addition, very sharp peaks at 2θ = 32.958° that observed at 3, 5, 6 Pa, are attributed to the forbidden reflection of Si substrate which occasionally appear in XRD measurement. It was observed that all the films deposited below 10 Pa exhibited strong AlN (002) diffractions, which indicates the preferential c-axis orientation of AlN perpendicular to the film surface. Neither aluminum nor metastable zincblende phase was found, which indicates no large N deficiency occurs and synthesized films have a wurtzite structure. The changes of peak intensities and full-width-half-maximum (FWHM) of AlN (002) peak have been plotted in Figure 2. Apparently, the intensity of (002) peak keeps increasing from 0.2 Pa to 0.9 Pa, however it starts to decrease after it reached the highest value at 0.9 Pa. In addition, FWHM of (002) peak keeps decreasing from 0.2 Pa to 0.9 Pa and starts to increase after 0.9 Pa, showing the same trend with the variation of (002) peak intensity. At

ACCEPTED MANUSCRIPT

higher N_2 pressure (10 Pa), instead of (002) peak, the XRD patterns showed only AlN (100) diffraction. The preferred orientation changes from (002) to (100) at 10 Pa indicating the c-axis of AlN crystallites changes from perpendicular to parallel with respect to substrate surface. The AlN (100) peak intensity keeps decreasing with further increasing N_2 pressure (over 10 Pa). Judging from XRD result, the highest intensity and lowest FWHM of AlN (002) peak at 0.9 Pa reflects the optimal crystal growth condition for c-axis-oriented AlN at this N_2 pressure and the preparation condition window is very narrow.

The film thickness was estimated using a surface profilometer by measuring the step fabricated with a mask on the substrate during the deposition. Figure 3 shows the calculated deposition rate at various N_2 pressures. The highest deposition rate is achieved at 0.9 Pa, implying the fastest growth rate along c-axis. Above the pressure, the deposition rate rapidly decreases with increasing the N_2 pressure.

Morphology

The cross-sectional SEM image of the highly-oriented AlN film deposited at 0.9 Pa is shown in Figure 4. The inset shows the interface situation between AlN film and substrate. It is clear that the AlN thin film exhibits numerous columnar grains which are perpendicular to the surface of substrate. Besides, the SEM image also suggests a formation of an amorphous starting layer between AlN and native oxide of Si layers. Such amorphous layer was observed by C.M. Lin et al. as well in epitaxial growth of AlN on 3C-SiC (100) by reactive magnetron sputtering [24]. The amorphous starting layer in our case is slightly thicker than theirs. The nature of natively-oxidized Si

ACCEPTED MANUSCRIPT

substrate is speculated to increase the thickness of such amorphous starting layer. Surface morphology and surface roughness of AlN films have been examined by using the SPM in atomic force microscopy (AFM) mode. Figure 5 shows the three-dimensional AFM surface morphology of AlN films in a 3×3 μm^2 area with a fixed Z-scale of 30 nm. Samples deposited from 0.2 Pa to 10 Pa are selected to display. From the AFM observation, all the films display uniform and crack-free surface. On the other hand, the root-mean-square (RMS) roughness is shown in Figure 6. It is observed that the surface roughness is drastically decreasing with the increasing N_2 pressure. The RMS roughness passes though a minimum value of 0.561 nm at 5 Pa, which is comparable to the substrate roughness.

Discussion on evolution of preferred orientation and growth rate

The evolution of preferred AlN orientation with the N_2 pressure has been discussed a lot in AlN deposition by sputtering [25-27]. The N_2 pressure and Ar^+ sputtering yield are two factors that mainly affect the film preferred orientation in sputtering. However, as only pure N_2 gas was used in PLD, the corresponding explanation is quite different with sputtering. There is scarcely any report regarding the evolution of AlN preferred orientation in PLD and here we are trying to give out a reasonable explanation. It should be noted that the present growth mechanism can be discussed without consideration of epitaxial nature from the substrate because the present substrate is natively oxidized Si.

From the results of Figs.2 and 3, the (002) preferential orientation and the deposition rate are found to have a strong correlation, suggesting that the large

ACCEPTED MANUSCRIPT

deposition rate enhances the (002) preferential orientation. In general, this phenomenon is well known as the deposition-rate-dependent preferential orientation. Supposing there are two competitive growth planes with a large and a small surface energy, the large surface energy plane is dominant in a large deposition rate case while two planes are competitive in a small deposition rate case. In other words, the crystals with a small surface energy cannot survive in a large deposition rate while those can survive in a small deposition rate. However, the surface energy of AlN is quite controversial according to the published literatures [28-33]. Most of the papers on growth of AlN nanostructures and AlN films are showing AlN (002), i.e. c-axis orientation, suggesting AlN (002) plane has the largest surface energy. The evaluation of AlN surface energy and the expected growth rate in terms of dangling bond density and consideration of polarization has been shown in Table I. The consideration of polarization is believed to be crucial to determine AlN surface energy. Actually, the top/bottom surfaces of the ± (001) dominated AlN films would be charged with positive and negative charges by polarization due to its noncentral symmetry structure. Hence, AlN (002) plane possesses larger surface energy than AlN (100) plane and is easier to be formed at low N_2 pressure with higher deposition rate.

Let us discuss on the N_2 pressure dependence of deposition rate and the crystal orientation in detail. As known, the AlN (002) plane is the close-packed plane and the AlN (100) plane is the loose-packed plane [34]. For formation of close-packed AlN (002) plane, sufficient kinetic energy of depositing species is essential to rearrange the adatoms on the surface. As stated previously in the section of introduction, energetic

ACCEPTED MANUSCRIPT

ACCEPTED MANUSCRIPT

species can be achieved in PLD. At low pressure, such energetic species will not face much resistance of the environment, which are energetically favorable for the formation of close-packed AlN (002) plane. At higher N_2 pressure (over 0.9 Pa), laser ablated species will collide with N_2 gas molecules lowering the species energy in the plume. Therefore, a decrease in deposition rate is observed. According to the reduced energy of laser ablated species with increasing N_2 pressure, the deposition rate should also continuously decrease with increasing N_2 pressure. However, it shows an elevating deposition rate at low N_2 pressure (from 0.2 Pa to 0.9 Pa). Confinement of laser plume is introduced to explain this discrepancy. At low N_2 pressure, ablated species are spreading with a wide solid angle as well, which is good to large-area deposition, but brings a lower deposition rate at the same time. By the admission of N_2 gas up to an appropriate pressure, the deposition rate could be greatly elevated by a confined plume, i.e. a thin plume. Consequently, the film deposited at low N_2 pressure like 0.2 Pa has (002) preferred orientation but lower deposition rate. At higher N_2 pressure like 10 Pa, the energy of laser ablated species are further weakened and become insufficient to form close-packed (002) plane. Instead, more loosely packed AlN (100) is formed resulting in preferred orientation changed from (002) to (100). The optimal N_2 pressure to achieve the highest deposition rate was 0.9 Pa.

Conclusion

PLD can be utilized to grow highly c-axis-oriented AlN films directly on natively-oxidized Si substrate. N_2 pressure was found to be a crucial parameter in controlling preferred orientation. Low N_2 pressure was favorable to form (002)

ACCEPTED MANUSCRIPT

ACCEPTED MANUSCRIPT

preferred orientation. With increasing N_2 pressure, it changed from (002) to (100) indicating the c-axis of AlN crystallites changes from perpendicular to parallel with respect to substrate surface. Pressure-controlled PLD growth can also be actively utilized to design the surface morphology of AlN films. Surface roughness is found to be drastically decreasing with the increasing N_2 pressure. Sample deposited at 0.9 Pa is experimentally proved to have the highest (002) peak intensity, the lowest FWHM value, the highest deposition rate and relatively low RMS roughness (1.138 nm), showing the optimal growth condition for c-axis-oriented AlN growth. The deposition-rate-dependent preferential orientation, kinetic energy of depositing atoms and the confinement of laser plume were introduced to explain the evolution of preferred orientation and deposition rate.

References

[1] W.M. Yim, E.J. Stofko, P.J. Zanzucchi, J.I. Pankov, M. Ettenberge, S.L. Gilbert, J. Appl. Phys. 44 (1973) 292.

[2] S. Strite, H. Morko¸c, J. Vac. Sci. Technol. B 10 (4) (1992) 1237.

[3] C. Jimenez, S. Gilles, P. Doppelt, C. Bernard, R. Madar, Surf.Coat. Technol. 76-77 (1995) 372.

[4] X.H. Xu, H.S. Wu, C.J. Zhang, Z.H. Jin, Thin Solid Films 388 (2001) 62-67.

[5] T. Aubert, O. Elmazria, B. Assouar, L. Bouvot, M. Oudich, Appl. Phys. Lett. 96, 20 (2010).

[6] G. Wingqvist, Surf. Coat. Tech. 205, 5 (2010).

[7] G. Piazza, P. J. Stephanou, and A. P. Pisano, J. Microelectromech. Syst. 15, 1406

ACCEPTED MANUSCRIPT

(2006).

[8] J. Bjurström, I. Katardjiev, and V. Yantchev, Appl. Phys. Lett. 86, 154103 (2005).

[9] C.M. Lin, T.T. Yen, Y.J. Lai, V. V. Felmetsger, M. A. Hopcroft, J. H. Kuypers, and A. P. Pisano, IEEE Trans. Ultrason. Ferroelectr. Freq. Control 57, 524 (2010).

[10] I. Yonenaga, Physica B 308−310 (2001) 1150−1152.

[11] C. Caliendo, P. Imperatori, Appl. Phys. Lett. 83 8 (2003).

[12] I. Tang, H. Chen, W.C. Hwang, Y.C. Wang, M. Houng, Y. Wang, Journal of Crystal Growth 262 (2004) 461−466.

[13] M.B. Assouar, O. Elmazria, R. Jimenez Rioboo, F. Sarry, P. Alnot, Appl. Surf. Sci. 164 (2000) 200–204.

[14] G.F. Iriarte, F. Engelmann, I.V. Katerdjiev, J. Mater. Res. 17 (2002) 1469.

[15] H. Nakahata, A. Hachigo, K. Higaki, S. Fujii, ,S. Shikata, N. Fujimori, IEEE Trans. Ultrason. Ferroelectr. Freq. Control, 42 2 (1995).

[16] J. Dupuie, E. Gulari, J. Vac. Sci. Technol. A 1992 (10) 18–28.

[17] Z. Sitar, L. Smith, R. Davis, J. Crys. Growth 1994 (141)11–21.

[18] X. Yan, Y. Dong, H. Li, J. Gong, C. Sun, Mater. Lett. 64 (2010) 1261–1263

[19] T. Shiosaki, T. Yamamoto, T. Oda, A. Kawabata. Appl. Phys. Lett. 1980 (36) 643–5.

[20] D.B. Chrisey and G.K. Hubles (eds.), Pulsed laser deposition of thin films, New York, 1994; and references cited therein.

[21] W.M. Yim, R.J. Paff, J. Appl. Phys. 45 (1974) 1456.

[22] .G. Carlotti, G. Gubbiotti, F.S. Hickernell, H.M. Liaw, G. Socino, Thin Solid Films

ACCEPTED MANUSCRIPT

310 (1997) 34.

[23] M. He, N. Cheng, P. Zhou, H. Okabe, J. B. Halpern, J. Vac. Sci. Technol. A 16(4) 1998.

[24] C.M. Lin, W.C. Lien, V. V. Felmetsger, M. A. Hopcroft, D. G. Senesky, A. P. Pisano, Appl. Phys. Lett. 97, 141907 (2010).

[25] H. Cheng, Y. Sun, J.X. Zhang, Y.B. Zhang, S. Yuan, P. Hing, Journal of Crystal Growth 254 (2003) 46 – 54.

[26] H. Cheng, P. Hing, Surf. Coat. Tech. 167 (2003) 297-301.

[27] K.H. Chiu, J. H. Chen, H.R. Chen, R.S. Huang, Thin Solid Films 515 (2007) 4819 – 4825.

[28] R.D. Vispute, J. Narayan, J.D. Budai, Thin Solid films 299 (1997) 94-103.

[29] C. D. Lee, Y. Dong, and R. M. Feenstra, Phys. Rev. B 68, 205317 (2003).

[30] K. S. Stevens, A. Ohtani, M. Kinniburgh, and R. Beresford, Appl. Phys. Lett. 65 (3) 1994.

[31] H.B. Li , R. Wu, J. Li, Y.F. Sun, Y.F. Zheng, J.K. Jian, J. Alloy. Compd. 509 (2011) 2111–2115.

[32] S. C. Shi, S. Chattopadhyay, C.F. Chen, K.H. Chen, L.C. Chen, Chem. Phys. Lett. 418 (2006) 152–157.

[33] L Yu, Y. Lv, P. Liu, X. Yu, Mater. Lett. 65 (2011) 1499-1502.

[34] H.L. Kao, P.J. Shih, C.H. Lai, Jpn. J. Appl. Phys. 38 (1999) 1526.

ACCEPTED MANUSCRIPT

Figure 1. XRD patterns of AlN films deposited at various N_2 pressures.

Figure 2. Variation of XRD peak intensities of AlN films deposited at various N_2 pressures.

Figure 3. Film thickness and deposition rate vs. N2 pressure for AlN films.

Figure 4. Cross-sectional SEM image of the AlN film deposited at 0.9 Pa. The inset shows interface between AlN film and Si substrate.

Figure 5. AFM images of AlN films prepared at various N_2 pressures. Scanning area: 3 μm × 3 μm; Z-Max: 30 nm.

Figure 6. RMS roughness vs. N_2 pressure for AlN films obtained from AFM scans in Figure 5.

Table I Evaluation of AlN surface energy and corresponding growth rate.

ACCEPTED MANUSCRIPT

ACCEPTED MANUSCRIPT

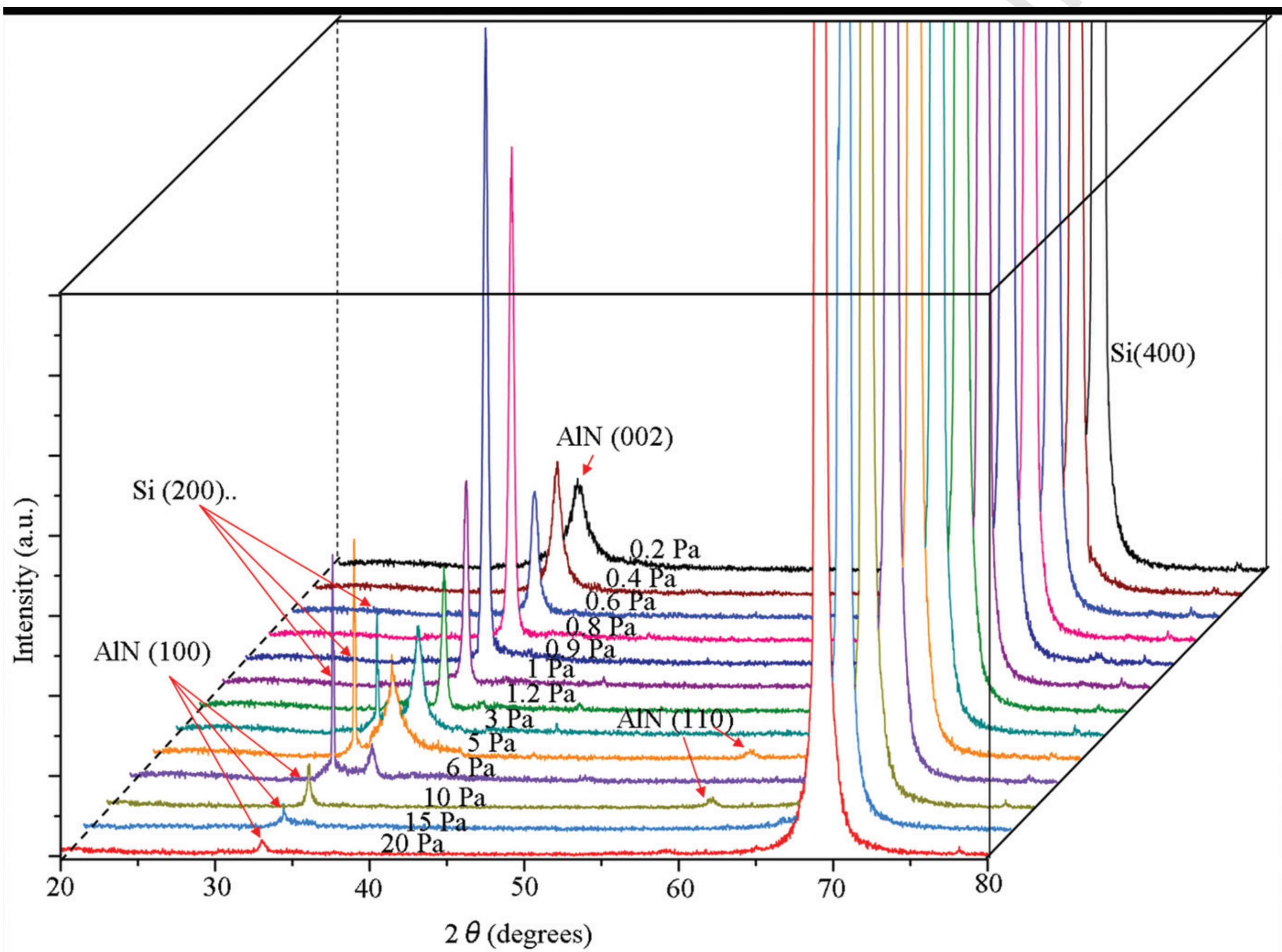

Figure 1

ACCEPTED MANUSCRIPT

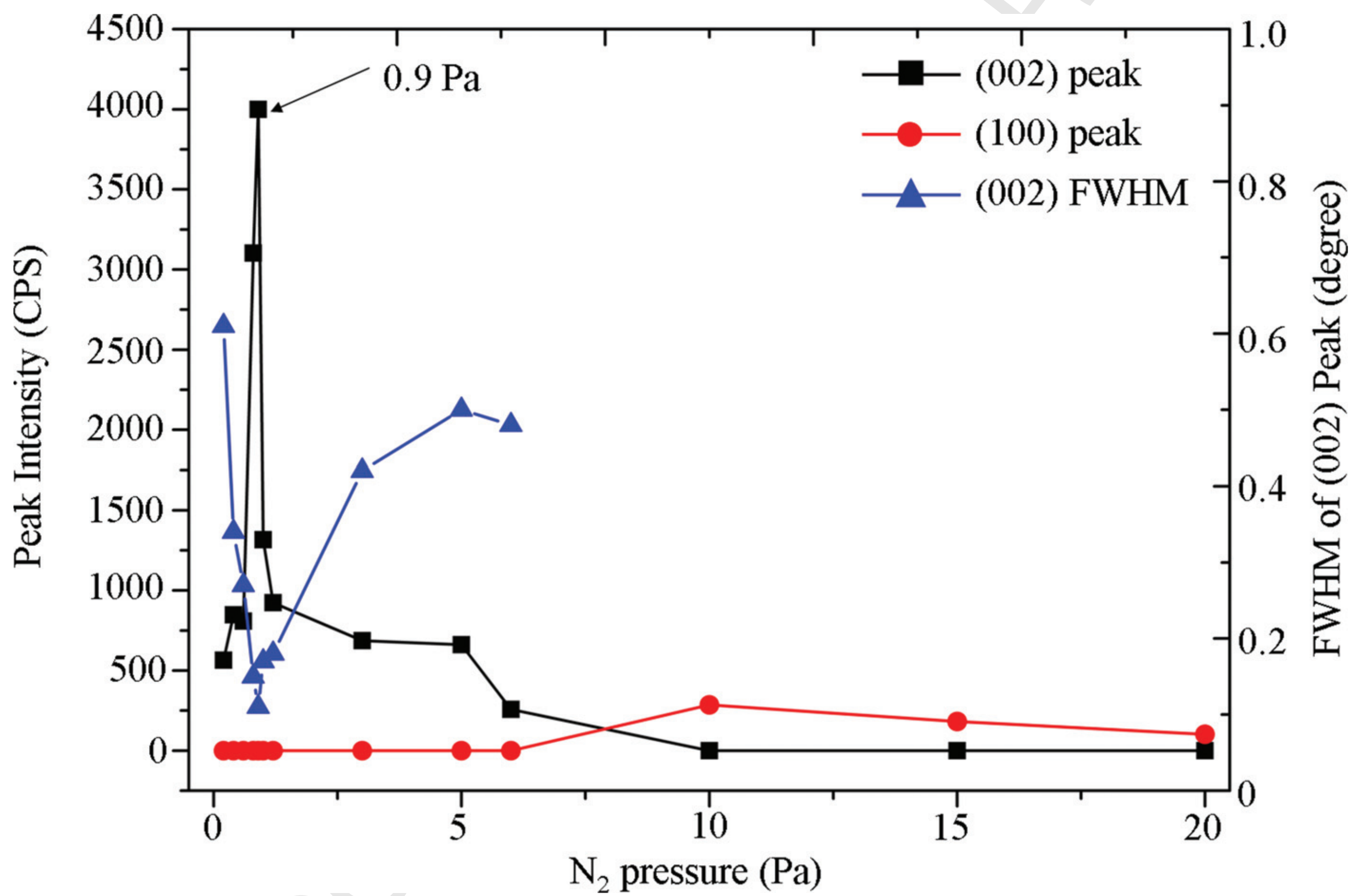

Figure 2

ACCEPTED MANUSCRIPT

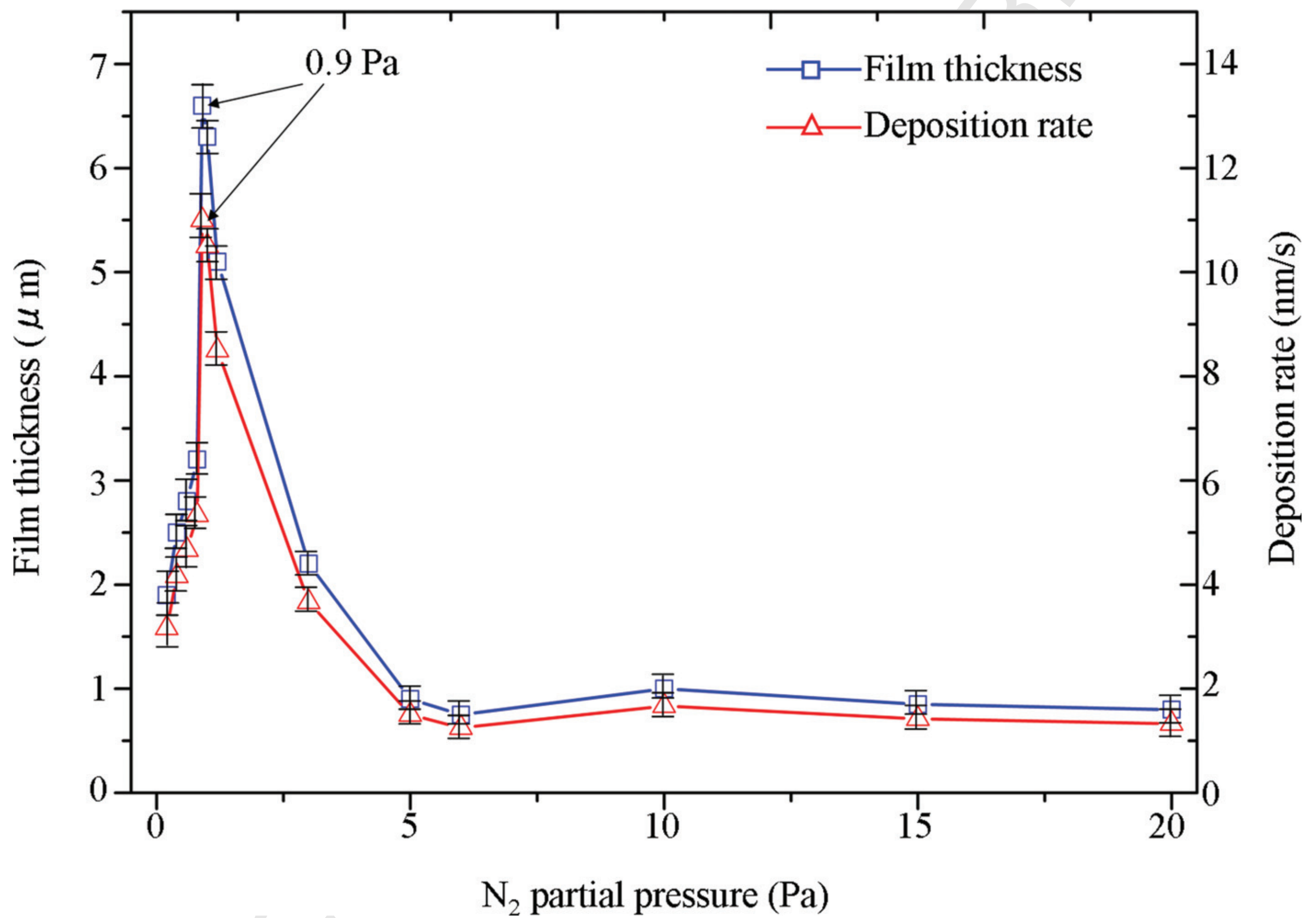

Figure 3

ACCEPTED MANUSCRIPT

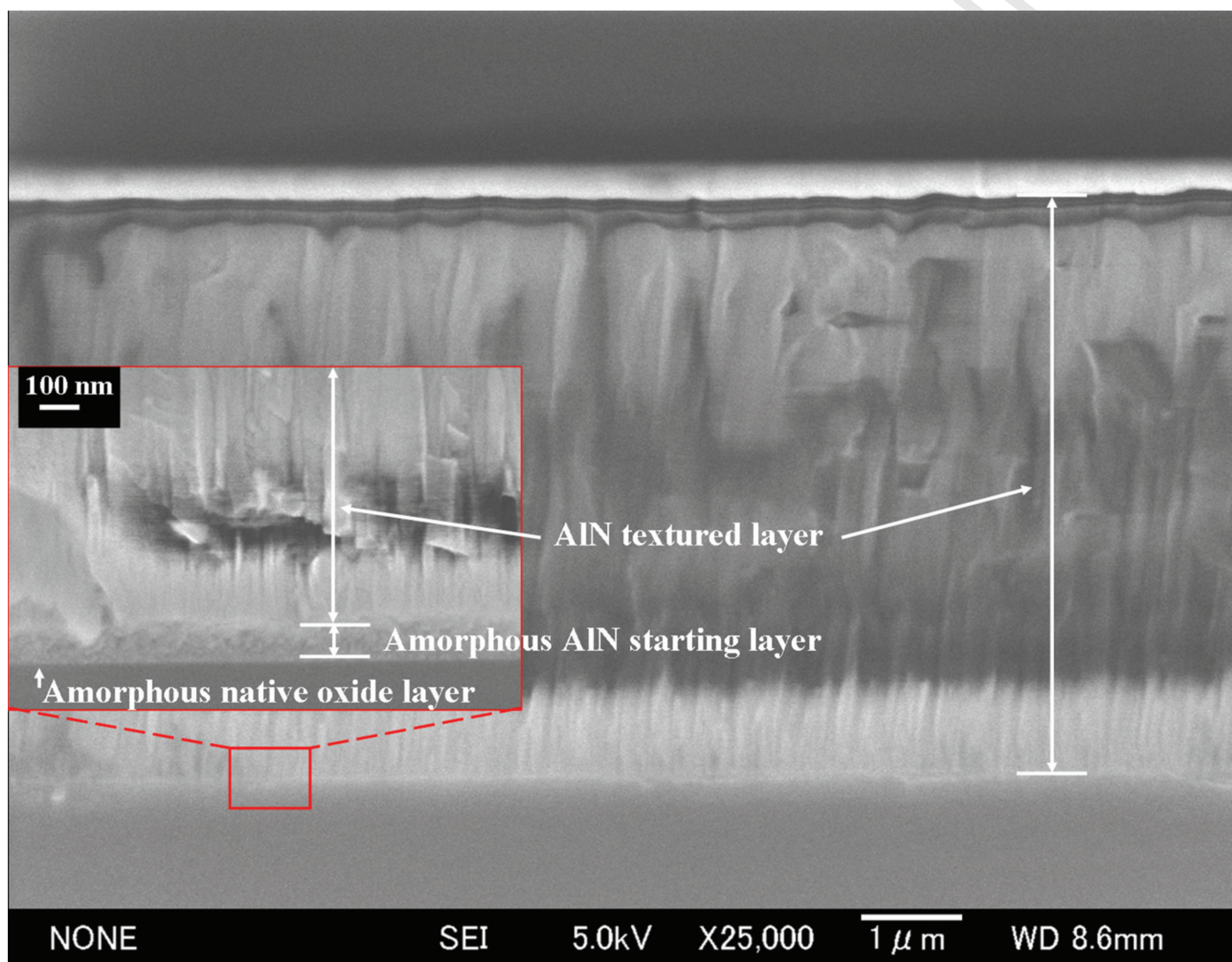

Figure 4

ACCEPTED MANUSCRIPT

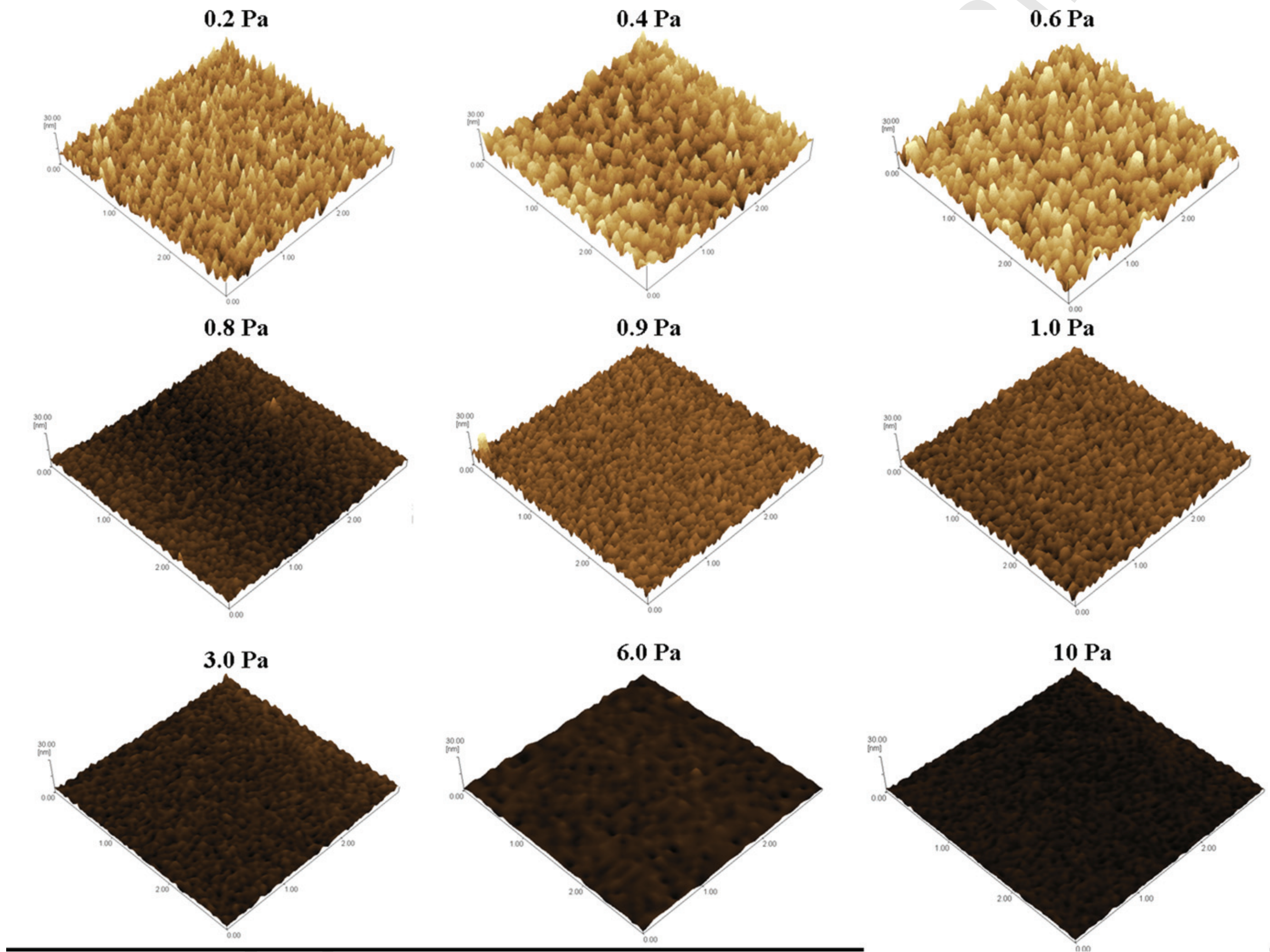

Figure 5

ACCEPTED MANUSCRIPT

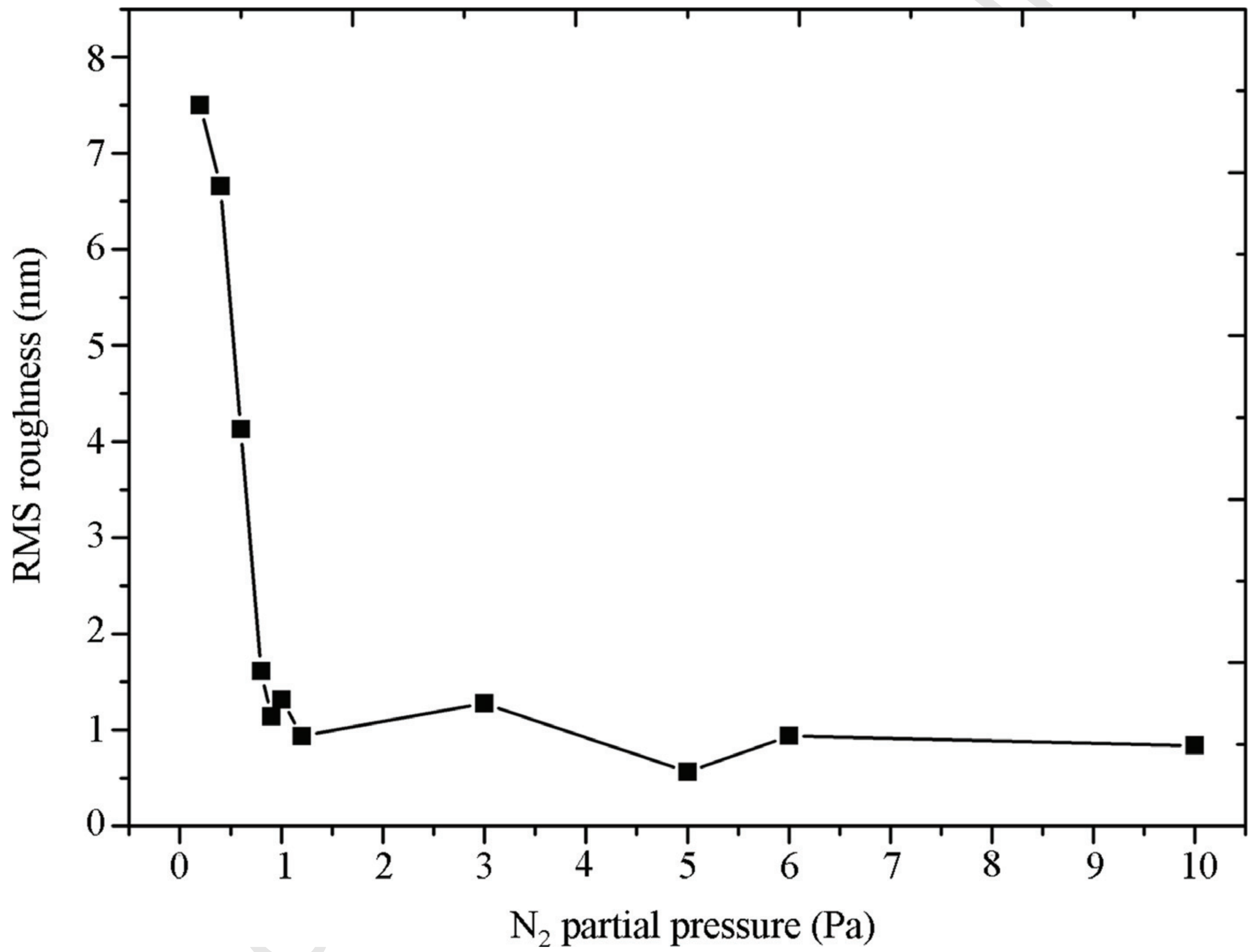

Figure 6

ACCEPTED MANUSCRIPT

		(002)	(100)	(110)
No consideration of polarization	Dangling bond density [bonds/cm^2]	11.94×10^{14}	12.91×10^{14}	14.91×10^{14}
	Surface energy	Small	Medium	Large
	Expected growth rate	Small	Medium	Large
Consideration of polarization	Surface energy	Large	Small	Medium
	Expected growth rate	Large	Small	Medium

ACCEPTED MANUSCRIPT